JOURNAL OF Materials CHEMISTRY

A hydrothermal post-synthesis route for the preparation of high quality MCM-48 silica with a tailored pore size

Ji-Hong Sun and Marc-Olivier Coppens*

Reactor and Catalysis Engineering, DelftChemTech, Delft University of Technology, Julianalaan 136, 2628BL Delft, The Netherlands. E-mail: M.O.Coppens@tnw.tudelft.nl

Received 12th June 2002, Accepted 18th July 2002
First published as an Advance Article on the web 16th August 2002

A post-synthesis hydrothermal restructuring method is introduced as a convenient route to synthesize high quality MCM-48 silica with controllable pore size. Using tetraethyl orthosilicate as the silica source and cetyltrimethylammonium bromide (CTAB) as the template, the pore size could be tailored from 2.6 to 4.2 nm without using organic additives other than CTAB. It was shown by means of nitrogen adsorption, X-ray diffraction, transmission electron microscopy, and scanning electron microscopy that the improved long range structural order and the expanded pore size of the materials depends on the treatment conditions, such as the CTA^+ concentration, the amount of NH_4OH added, and the aging temperature during the post-synthesis procedure.

1 Introduction

MCM-48 is a nanoporous silica with a periodic, three-dimensional array of separate channels. Its structure is cubic bi-continuous and belongs to the space group *Ia3d*.[1–3] Both MCM-41 and MCM-48 are of potential interest for catalysis and for optical and electronic applications. However, compared to the more familiar MCM-41 (and SBA-15), with its one-dimensional hexagonal array of pore channels, MCM-48 provides easier access to guest molecules due to its three-dimensional pore network. This decreases diffusion limitations and makes MCM-48 more resistant to pore blocking if the pores are wide enough.[3] Despite this advantage over MCM-41 and SBA-15, the synthesis of high quality MCM-48 with controlled pore size is more challenging. The classic surfactants used in the synthesis of the M41S family are the alkyltrimethylammonium halides, like CTAB, which preferentially form hexagonal (MCM-41) or lamellar (MCM-50) mesophases, implying that the synthesis of high quality MCM-48 is only possible within a very narrow window of synthesis conditions and is often poorly reproducible.[4,5]

Generally, MCM-48 materials have been obtained *via* a hydrothermal route by using a high surfactant to silica ratio, and mainly changing the pH of the reaction medium, the catalyst, the reaction time, and the temperature.[5–8] To obtain high quality, large pore MCM-48 materials, new synthesis approaches based on the conventional route were developed. Recently, it has been reported that post-synthesis treatment and tailoring the alkyl chain length of the cationic surfactant by using mixtures of cationic–anionic[9] and cationic–neutral surfactants[10,11] lead to increased pore size in MCM-48. Meanwhile, gemini surfactants[12–15] added as swelling agents to the synthesis gel were found to favor the formation of MCM-48 with enlarged pores by adjusting the different surfactant chain lengths. In all cases, the pore size of the good quality MCM-48 silica was in the range 2–3.2 nm, and even 3.8 nm on one very recent occasion.[15] Also recently, high quality MCM-48 with a pore size of up to 3.8 nm (calculated by using the KJS model on the basis of the desorption branch of the nitrogen isotherm) was synthesized using fumed silica and without organic additives.[16]

Here, we report on a new, reproducible method using only CTAB to synthesize high quality MCM-48 with increased long range order and a tunable pore size up to at least 4 nm. The essence of this method is a post-synthesis hydrothermal restructuring route, inspired by our previous work in which the pore size of SBA-15 was enlarged by an alcothermal post-synthesis route, while simultaneously maintaining the pore wall thickness and increasing the long range order.[17]

2 Experimental

2.1 Synthesis method

The synthesis consists of two steps.

In the first step, cetyltrimethylammonium bromide (CTAB) was added to a mixture of deionized water and ethanol. Aqueous ammonia and tetraethyl orthosilicate (TEOS) were subsequently added at room temperature. The composition of the synthesis mixture was as follows: $TEOS : CTAB : H_2O :$ ethanol : $NH_4OH = 1 : 0.4 : 174 : 54 : 12.5$ (molar ratio), similar to the procedure described by Schumacher *et al.*[7] After stirring the mixture continuously for 5 h at room temperature, it became a white gel. This gel was filtered using a Büchner funnel and repeatedly washed with distilled water.

In the second step, the white gel was divided into two parts. One part was dried at 120 °C for 3 h, and subsequently calcined in air by heating at a rate of 5 °C min^{-1} to 550 °C and maintaining this temperature for 6 h, leading to the "primary" MCM-48 material (sample 1). Another part was immersed in water containing different amounts of CTAB (0–4 wt%). The resulting gels were aged for 48 h in an autoclave at the desired temperature. Finally, the products were filtered and washed with distilled water. After drying and calcination in a manner similar to the procedure followed for the primary gel, a series of "secondary" MCM-48 materials was formed. The standard case (sample 2), which we will discuss first, corresponds to an aging temperature of 100 °C, 2 wt% of CTAB, and pH 8.5 during the second synthesis step.

2.2 Characterization

Powder X-ray diffraction (XRD) studies were performed using a Philips XRD spectrometer (PW1840) with Cu-$K_{\alpha 1}$ radiation, operating at 40 kV and 50 mA. Nitrogen adsorption–desorption isotherms were measured with a Micromeritics ASAP2000 sorption analyzer, utilizing the Broekhoff–de Boer (BdB) method to evaluate the pore volume and pore size

 DOI: 10.1039/b205646a

This journal is © The Royal Society of Chemistry 2002

distributions from the desorption portion of the isotherms. This method has been shown to be reliable for materials with narrow mesopores.[18] The pH value of the solution was measured using pH paper. Transmission electron micrographs (TEM) were obtained with a JEOL JEM 4000-EX electron microscope operating at 400 kV. The sample was dispersed in acetone, and then deposited and dried on a holey carbon Cu grid. Scanning electron micrographs (SEM) were recorded using a Philips XL20 microscope operated at an accelerating voltage of 20 kV and a 100–200 μA current. Samples were deposited on a sample holder with an adhesive carbon foil and sputtered with gold.

3 Results and discussion

3.1 Characterization of sample 2: a high quality MCM-48 with large pore size

The XRD patterns of the calcined samples show the characteristic cubic order of MCM-48 (Fig. 1).[1,2] The XRD pattern of the secondary material (sample 2, *i.e.* the standard case) shows a significantly increased intensity for the (211) peak compared to the primary material (sample 1), as well as three higher order (220), (420), and (332) peaks. In addition, there are seldomly observed (321), (400), (422), and (431) peaks.[15,16,19] The reflections from sample 2 are more intense than those of sample 1, indicating that the degree of order has improved. Meanwhile, the d_{211} spacing of sample 2 increased from 3.1 to 3.9 nm, suggesting increased unit cell parameters, as can be seen in Table 1.

The nitrogen adsorption isotherms and corresponding pore size distributions (Fig. 2) indicate that the mesopore size has increased from 2.6 nm to 3.7 nm, most likely by swelling of the organic structure-directing entities in the primary material.[17,20] The sharpness of the nitrogen condensation step (P/P_0 = 0.3–0.4) and the well-defined XRD peaks provide strong evidence of the very high quality of sample 2. The hysteresis loop of this sample at a relative pressure P/P_0 = 0.45–0.9 is due to interparticle porosity.

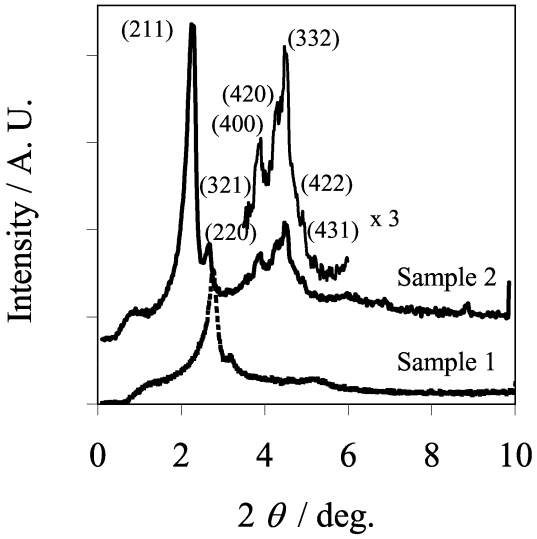

Fig. 1 XRD patterns of MCM-48. Sample 1: primary MCM-48; sample 2: secondary MCM-48.

Table 1 Pore structure parameters of MCM-48 materials

Sample	Aging temp./°C	a^a/nm	S^b/m^2 g^{-1}	V^c/cm^3 g^{-1}	D^d/nm	H^e/nm
1		7.75	1510	0.74	2.6	1.2
2	100	9.53	1170	1.24	3.7	1.2
3	60	8.54	1470	0.94	3.2	1.2
4	150	12.3	740	0.78	4.2	1.9

$^a a = d_{hkl}(h^2 + k^2 + l^2)^{1/2}$ is a cubic lattice parameter calculated from XRD. $^b S$ is the specific surface area obtained from nitrogen adsorption and desorption. $^c V$ is the specific pore volume. $^d D$ is the mean pore diameter. $^e H = a/3.092 - D/2$ is the mean pore wall thickness.

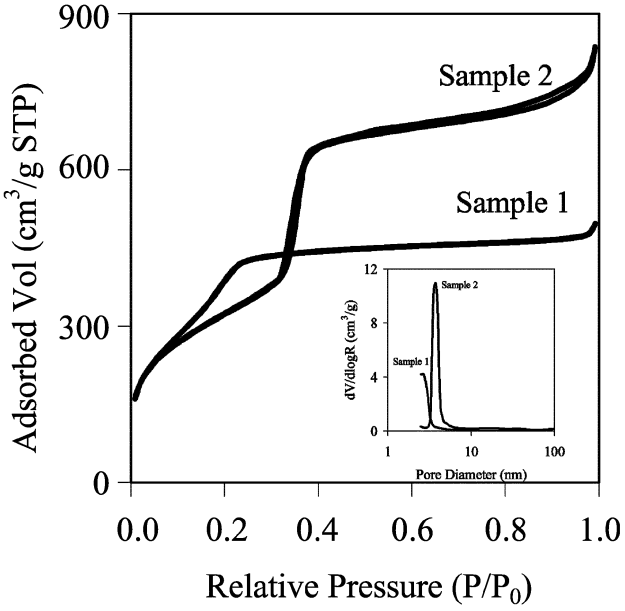

Fig. 2 Nitrogen adsorption isotherms and corresponding pore size distributions of the primary and secondary MCM-48.

TEM confirms the high degree of cubic order of the secondary MCM-48 sample 2 (Fig. 3). Along the [110] direction [Fig. 3(a)], a very regular pattern is clearly observed, while along the [100] direction [Fig. 3(b)]. the image shows a uniform square pore network arrangement, characteristic of MCM-48.[5]

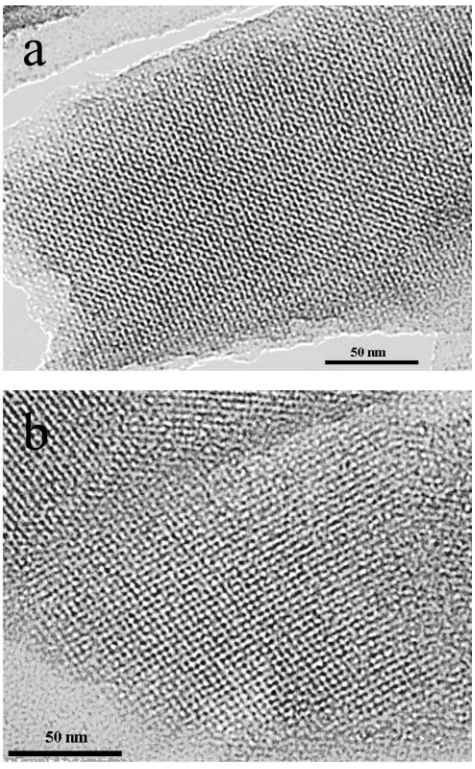

Fig. 3 TEM images of secondary MCM-48 (sample 2) recorded along the (a) [110] and (b) [100] directions.

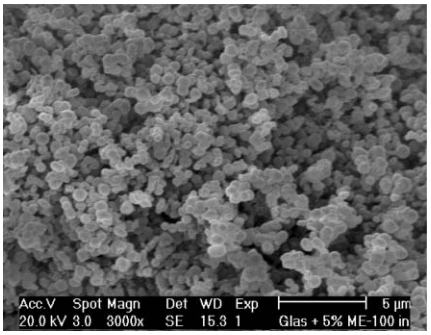

Fig. 4 SEM image of secondary MCM-48 (sample 2).

The SEM image in Fig. 4 shows non-agglomerated particles, very uniform in size (around 1.0–1.3 μm), and near spherical in shape. A closer look reveals the unique crystalline morphology of cubes truncated by a rhombic dodecahedron, typical for MCM-48.[19]

Table 1 summarizes the textural characteristics of the primary and secondary MCM-48 materials. From the XRD and the nitrogen isotherm adsorption data, the pore wall thickness, H, can be estimated. The highly ordered secondary MCM-48 (sample 2) has a pore wall thickness of approximately 1.2 nm, unchanged from that in the primary MCM-48 (sample 1). This indicates that the unit cell enlargement can be almost entirely attributed to an increase in pore size. The surface area remains well above 1000 $m^2\ g^{-1}$ and the pore volume increases due to the pore size expansion.

3.2 Effect of the amount of CTAB added during the second synthesis step

A post-synthesis treatment can rearrange the structure or change the properties of mesoporous silicas, the main reason being that the as-prepared mesophases are still flexible after the primary synthesis step.[17,20] The effect of post-synthesis hydrothermal treatment depends on the conditions during this treatment.

When the concentration of CTAB is increased during the second synthesis step in basic media, the crystallinity of the MCM-48 silicas goes through an optimum, as shown *via* the XRD patterns of calcined secondary samples in Fig. 5. The cubic mesostructure is stable with increased concentrations of CTAB from 0 to 2 wt%, while the position of the (211) cubic diffractogram peak is gradually shifted to a lower diffraction angle. When the CTAB concentration is further increased to a value of 4 wt%, the XRD patterns suggest that a mixture of mesoporous particles is obtained (*viz*. the two intense peaks close to $2\theta = 2^\circ$). This could be explained by a mesophase transition during the second synthesis step, as a result of a cooperative templating mechanism.[5,21] The self-assembly of the organic–inorganic interface can be qualitatively predicted by the value of the surfactant packing parameter, $g = V/(a_0L)$, where V is the total volume of surfactant chain, a_0 is the effective headgroup area at the micelle surface, and L is the kinetic length of the alkyl chain. A cubic mesophase (*Ia*3*d*) forms for g-values in the interval 0.5–0.65, whereas a hexagonal phase or a lamellar phase form at g-values below 0.5 or above 0.65.[11,22] Obviously, the effective surfactant volume, V, is increased when the amount of CTAB is raised during the second synthesis step, resulting in an increased value for the packing parameter, g.[23] The best MCM-48 silica was obtained for 2 wt% CTAB (standard case, sample 2), while variations around this amount reduce the crystallinity (less than 2 wt% CTAB) or result in a mixture of mesophase solids, possibly MCM-48 and the lamellar MCM-50 (more than 2 wt% CTAB).[11,16,22]

3.3 Effect of the pH during the second synthesis step

The silicate framework in the primary gel contains a large amount of silanols, which can further condense and rearrange. Thus, when the silicate is only partially polymerized and is still flexible, it should be possible to transform the organic–inorganic composite materials (mesophases) from one M41S phase to another.[24] The post-synthesis treatment could rearrange the structure or change the properties of some mesoporous silica, which is sensitive to factors such as the pH of the environment. In Fig. 6, XRD patterns are shown for secondary MCM-48 calcined materials synthesized with different amounts of NH_4OH or HCl added during the second step. It is well known that an acidic or neutral environment (pH $\approx$ 7) favors the formation of a mixed mesophase, as is confirmed by the two peaks at low angles (pattern a in Fig. 6), suggesting that the MCM-48 phase has been partially transformed into another structure, possibly MCM-41.[25] When the amount of ammonium hydroxide is increased to $NH_4OH/H_2O \cong 0.0027$ (sample 2), corresponding to pH $\cong$ 8.5, the MCM-48 structure becomes the most favorable phase and is obtained in high yield,

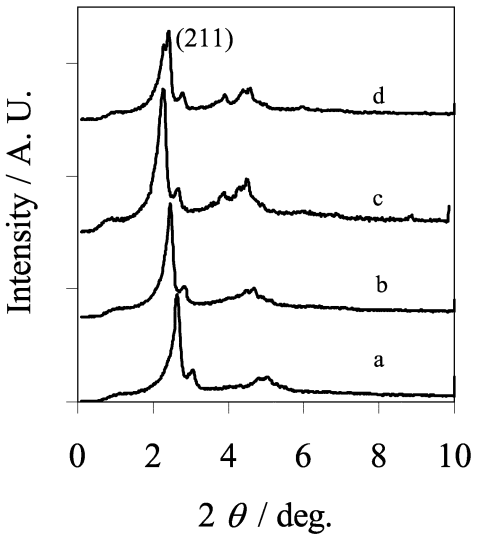

Fig. 5 XRD patterns of secondary MCM-48 samples synthesized by adding different amounts of CTAB during the second step: (a) 0; (b) 1; (c) 2; (d) 4 wt%.

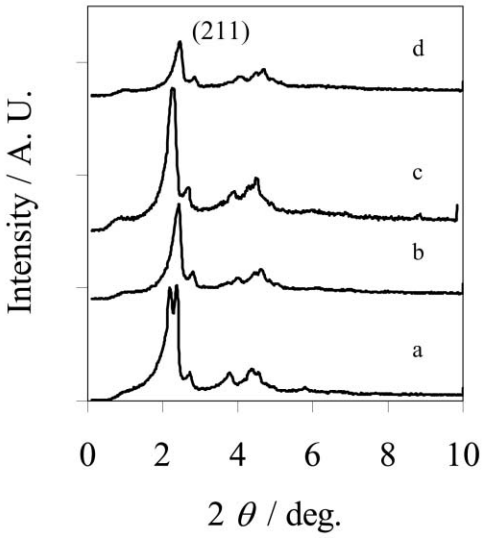

Fig. 6 XRD patterns of the secondary MCM-48 synthesized at different pH values during the second step: (a) $HCl/H_2O = 0.0054$ (pH 7.0); (b) $NH_4OH/H_2O = 0$ (pH 8.0); (c) $NH_4OH/H_2O = 0.0027$ (pH 8.5); (d) $NH_4OH/H_2O = 0.0081$ (pH 9.5).

as can be seen from the high intensity of the X-ray diffractogram peaks (pattern c in Fig. 6). Further increasing the amount of ammonium hydroxide leads to a decrease in the quality of the MCM-48: comparing patterns c and d in Fig. 6 reveals that the latter has lower diffractogram intensities and a smaller unit cell parameter (8.8 instead of 9.5 nm).

The influence of the basicity of the environment on the phase formation and phase transitions can be explained as follows.[23] The formation of highly negatively charged silicate oligomers is promoted by increasing the amount of ammonium hydroxide present during the second synthesis step, and this has to be compensated for by the CTA^+ cations. This promotes self-assembly and the formation of an ordered phase. But when the amount of ammonium hydroxides is too high, the dissolution of the silicate framework is enhanced,[26] thereby continuously reducing the charge density interaction with the cationic surfactant.[5] As a result, the formation of an ordered mesophase as a function of pH has a distinct optimum point, where an ordered MCM-48 structure with expanded unit cell parameter is formed. In acid media, a mixture of phases is obtained.[25] A low pH value favors the formation of MCM-41, the main reason being that the ion pairing interaction between the silicate framework and the surfactant head groups is changed, thereby decreasing the surfactant packing parameter and redirecting the mesophase structure, leading to an MCM-41 mesophase.

3.4 Effect of the aging temperature during the second synthesis step

Fig. 7 shows the XRD pattern of the secondary MCM-48 silicas as a function of the aging temperature in a basic medium. It is clear from the peak intensities that the crystallinity of the MCM-48 goes through an optimum point as the temperature is increased, while the (211) cubic reflection shifts toward lower diffraction angles, *i.e.* toward a larger cubic unit cell (see also Table 1). The long range order of the pores increases when the hydrothermal treatment temperature is increased from 60 to 100 °C, after which it decreases again. Increasing the temperature accelerates the polymerization of the silicate framework and makes the surfactant molecules more mobile, which favors the formation of high quality MCM-48 silicas (compare patterns a and b in Fig. 7). Increasing the temperature beyond an optimum value of around 100 °C, on the other hand, results in the dissolution of the silica framework and changes the value of the packing parameter *g*.[27] The unit cell of these materials increases from 8.5 nm at 60 °C (sample 3) to 12.3 nm at 150 °C (sample 4). The BdB pore size distribution curves (Fig. 7, inset) of samples 2 (curve a) and 3 (curve b) show a narrow pore size distributions with average pore sizes of 3.2 and 3.7 nm, respectively. Sample 4, synthesized at 150 °C, has a slightly wider pore size distribution and a larger average pore diameter (around 4.2 nm), showing that the mesopores of MCM-48 silica synthesized at high temperature are not as uniform as at lower temperatures. Interestingly, the pore walls of this sample are thicker (around 1.9 nm) than those of the primary MCM-48 (sample 1) and also than those of typical high quality MCM-48 as reported in the literature (around 0.8–1.0 nm),[28] suggesting that a rearrangement of the silica framework has taken place at the high temperature during the second synthesis step.[29]

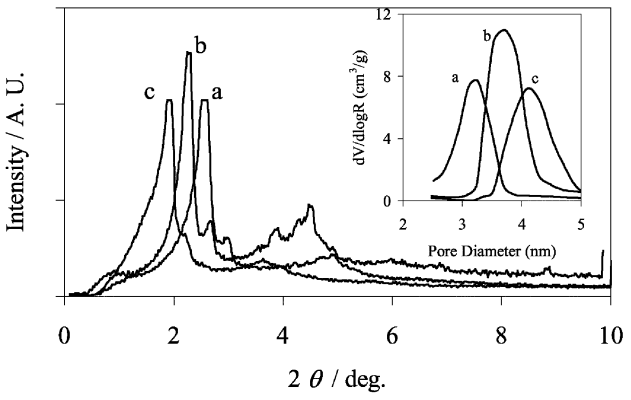

Fig. 7 XRD patterns and pore size distributions (inset) of secondary MCM-48 samples synthesized at different aging temperatures during the second step: (a) 60; (b) 100; (c) 150 °C.

4 Conclusions

It has been shown that restructuring a primary MCM-48 gel using CTAB *via* a hydrothermal post-synthesis method yields a secondary MCM-48 with pores that can be expanded from 2.6 to 4.2 nm, while increasing the degree of order (eight well-resolved diffraction peaks in the XRD pattern), maintaining thick pore walls at around 1.2 nm, and with a surface area typically well above 1000 $m^2\ g^{-1}$. The texture of the materials depends on the amount of CTAB, the basicity, and the aging temperature during the hydrothermal post-synthesis procedure. Optimal conditions to obtain large well-ordered samples are 100 °C, 2 wt% CTAB, pH 8.5, and aging for 48 h. This hydrothermal post-synthesis method provides a useful way to prepare high quality MCM-48 with controllable pore size.

Acknowledgements

We would like to thank Dr Chia-Min Yang for the TEM and Mr Johan C. Groen for measuring the nitrogen adsorption isotherms.

References

1 J. S. Beck, J. C. Vartuli, W. J. Roth, M. E. Leonowicz, C. T. Kresge, K. D. Schmitt, C. T.-W. Chu, D. H. Olson, E. W. Sheppard, S. B. McCullen, J. B. Higgins and J. L. Schlenker, *J. Am. Chem. Soc.*, 1992, **114**, 10834.
2 C. T. Kresge, M. E. Leonowicz, W. J. Roth, J. C. Vartuli and J. S. Beck, *Nature*, 1992, **359**, 710.
3 A. Monnier, F. Schuth, Q. Huo, D. Kumar, D. Margolese, R. S. Maxwell, G. D. Stucky, M. Krishnamurty, P. Petroff, A. Firouzi, M. Janicke and B. F. Chmelka, *Science*, 1993, **261**, 1299.
4 M. L. Pena, Q. Kan, A. Corma and F. Rey, *Microporous Mesoporous Mater.*, 2001, **44–45**, 9.
5 J. Xu, Z. Luan, H. He, W. Zhou and L. Kevan, *Chem. Mater.*, 1998, **10**, 3690.
6 J. C. Vartuli, K. D. Schmitt, C. T. Kresge, W. J. Roth, M. E. Leonowicz, S. B. McCullen, S. D. Hellring, J. S. Beck, J. L. Schlenker, D. H. Olson and E. W. Sheppard, *Chem. Mater.*, 1994, **6**, 2317.
7 K. Schumacher, M. Grun and K. K. Unger, *Microporous Mesoporous Mater.*, 1999, **27**, 201.
8 L. Z. Wang, J. L. Shi, J. Yu, W. H. Zhang and D. S. Yan, *Mater. Lett.*, 2000, **45**, 273.
9 R. Ryoo, S. H. Joo and J. M. Kim, *J. Phys. Chem. B*, 1999, **103**, 7435.
10 M. Kruk and M. Jaroniec, *Chem. Mater.*, 2000, **12**, 1414.
11 P. van der Voort, M. Mathieu, F. Mees and E. F. Vansant, *J. Phys. Chem. B*, 1998, **102**, 8847.
12 M. Benjelloun, P. van der Voort, P. Cool, O. Collart and E. F. Vansant, *Phys. Chem. Chem. Phys.*, 2001, **3**, 127.
13 M. Mathieu, E. van Bavel, P. van der Voort and E. F. Vansant, *Stud. Surf. Sci. Catal.*, 2001, **135**, 06-O-04.
14 M. Morey, S. O'Brien, S. Schwarz and G. D. Stucky, *Chem. Mater.*, 2000, **12**, 898.
15 M. Widenmeyer and R. Anwander, *Chem. Mater.*, 2002, **14**, 1827.
16 A. Sayari, *J. Am. Chem. Soc.*, 2000, **122**, 6504.
17 J. H. Sun, J. A. Moulijn, J. C. Jansen, T. Maschmeyer and M.-O. Coppens, *Adv. Mater.*, 2001, **13**, 327.
18 J. C. Groen, M. C. Doorn and L. A. A. Peffer, in *Adsorption Science and Technology, Proceedings of the Pacific Basin Conference on Adsorption Science and Technology*, ed. D. D. Do, World Scientific Publishing Co. Pte. Ltd., Singapore, 2000, p. 229.

19 J. M. Kim, S. K. Kim and R. Ryoo, *Chem. Commun.*, 1998, 259.
20 J. H. Sun and M.-O. Coppens, *Stud. Surf. Sci. Catal.*, 2002, in press.
21 Q. Huo, R. Leon, P. M. Petroff and G. D. Stucky, *Science*, 1995, **268**, 1324.
22 C. A. Fyfe and G. Fu, *J. Am. Chem. Soc.*, 1995, **117**, 9709.
23 A. A. Romero, M. D. Alba, W. Zhou and J. Klinowski, *J. Phys. Chem. B*, 1997, **101**, 5294.
24 K. W. Gallis and C. C. Landry, *Chem. Mater.*, 1997, **9**, 2035.
25 Y. Liu, A. Karkamkar and T. J. Pinnavaia, *Chem. Commun.*, 2001, 1822.
26 L. L. Hench and J. K. West, *Chem. Rev.*, 1990, **90**, 33.
27 Q. Huo, D. I. Margolese and G. D. Stucky, *Chem. Mater.*, 1996, **8**, 1147.
28 K. Schumacher, P. I. Ravikovitch, A. D. Chesne, A. V. Neimark and K. K. Unger, *Langmuir*, 2000, **16**, 4648.
29 D. Zhao and D. Goldfarb, *J. Chem. Soc., Chem. Commun.*, 1995, 875.